BIBLIOGRAPHIC INFORMATION SYSTEM

👁 **Vision:** Journal of Biomedical Research & Environmental Sciences main aim is to enhance the importance of science and technology to the scientific community and also to provide an equal opportunity to seek and share ideas to all our researchers and scientists without any barriers to develop their career and helping in their development of discovering the world.

ORIGINAL ARTICLE

PLGA Nanoparticles with Cannabidiol for Efficient and Durable Antibacterial Applications

Ming Cheng[1], Qiang Ma[1], Lu Tang[2], Bo Wang[2], Liya Liu[2], Bei Fan[2], Liang Zhang[1,2]* and Fengzhong Wang[2]*

[1]Institute of Environment and Sustainable Development in Agriculture, Chinese Academy of Agricultural Sciences, Beijing, China
[2]Institute of Food Science and Technology, Chinese Academy of Agricultural Sciences, Beijing 100193, China

Abstract

The Cannabidiol (CBD) are extensively used owing to their potent antibacterial effects. We developed CBD-loaded poly (lactic-co-glycolic acid) (PLGA) nanoparticles using an emulsion process technology, resulting informing the PLGA@CBD nanoparticles. The emulsion parameters were optimized using three-dimensional surface plots. When scaled up under optimal conditions, the corresponding loading content efficiency were 16.51%. Compared with natural cannabidiol, the physically modified PLGA nanoparticles became smooth, round, and solid, improving their water solubility and bioavailability, realizing long-time antibacterial. Therefore, the nanoparticles showed better efficacy against Gram-positive bacteria. Our results confirm that the PLGA@CBD nanoparticles have been achieved as long-acting antibacterial delivery system, which improved the treatment efficiency.

Introduction

Bacterial infections have become one of the major public safety events worldwide, causing serious threats to human health [1,2]. In clinical practice, the use of antibiotics remains the most common form of treatment for bacterial infections up to now [3]. However, the antibacterial effects are not great satisfaction to people of expectations because of the possible side effects, such as toxic reactions, drug resistance and so on [4,5]. Therefore, Drug Delivery Systems (DDSs) come into being and develop with the development of nanotechnology for delivering drugs into the site of the bacterial infection, achieving the objectives of extenuating the potential damage to the body and improving the therapeutic effectiveness [6-8].

Poly (lactic-co-glycolic acid) (PLGA) consists of Lactic Acid (LA) and Glycolic Acid (GA) monomers polymerized in the desired ratio, with good biodegradability and biocompatibility, it has also been approved by the US Food and Drug Administration (FDA) for medical applications [9,10]. It is used as a carrier for antimicrobial delivery, encapsulating the drug inside the carrier, protecting these agents from enzymatic and molecular damage and improving the therapeutic efficiency of the drug [11-13]. Moreover it can solve the problems of drug stability, solubility and bioavailability [12,14,15]. Thus PLGA as carrier, which can effectively solve the problems faced in drug delivery, have great potential for biomedical applications [16,17].

*Corresponding author(s)

Liang Zhang, Institute of Environment and Sustainable Development in Agriculture, Chinese Academy of Agricultural Sciences, Beijing, China

Tel: +86-106-281-0295
Email: zhangliang02@caas.cn

Fengzhong Wang, Institute of Food Science and Technology, Chinese Academy of Agricultural Sciences, Beijing 100193, China

Tel: +86-106-281-0295
Email: wangfengzhong@sina.com

Cannabidiol (CBD) is a purely natural component of the cannabis plant with anti-sedative, anti-psychotic and anti-anxiety effects and so on [18-20]. New cannabis-based medicines have recently undergone the rigorous testing required for regulatory drug approval, Sativex (a 1:1 mixture of Δ9-THC and CBD) in 2005 and Epidiolex in 2018 [21,22]. Moreover CBD is a powerful plant antibiotic with excellent antibacterial activity against gram-positive bacteria significantly [23]. Researchers have already demonstrated that found MIC values of CBD extracted from powdered plant material in the 0.5-2 μg/mL range towards various drug-resistant strains of *S. aureus* [24]. When CBD binds to bacteria, it disrupts cell membrane integrity by causing depolarization of the cytoplasmatic membrane [25]. However, one nearly universal truth is the case that the instability and hydrophobic property of CBD severely limit its potential contribution of applying in clinical treatment [26,27]. Thus, it is an important and urgent topic to search for CBD nanocarrier systems to address the challenge. The abovementioned PLGA could be a good choice and we incorporate CBD into the PLGA nanoparticles, which known as one of the most widely studied carriers and its high biological compatibility has also been confirmed.

The aim of the present study was to fabricate a practical delivery system to better cater to the clinical application of CBD. The CBD's inherent characteristics, biocompatibility of chosen materials, and complexity of preparation process were all taken into consideration for the design. In this contribution, we developed a simple but versatile procedure for improving the solubility and bioactivity of CBD by one-step encapsulating in PLGA compounds (defined as PLGA@CBD) during PLGA nanoparticles synthesis process.

Materials and Methods

Materials

Poly (lactic-co-glycolic acid) (PLGA) was bought Shandong Medical Device Research Institute. Cannabidiol (CBD) was purchased from Macklin. (Shanghai, China). Poly (vinyl alcohol) (PVA, Mw 47,000 Da, 98.0−98.8 mol% hydrolysis) was bought from Sigma-Aldrich (St. Louis, MO, USA). Other chemicals were of analytical grade.

Synthesis of PLGA@CBD nanoparticles

PLGA@CBD nanoparticles were prepared by the single emulsification and the nanoprecipitation techniques [28]. PLGA (200 mg) and CBD (40 mg) dissolved in 5ml of dichloromethane were mixed under ultrasonic processing for approximately 5 min and cautiously added dropwise, to the above 50 ml of 20 g/L poly (vinyl alcohol) (PVA) solution stirring at 1000 rpm for 30 min under an ice bath continuously. The mixture were then ultrasonic emulsified for 3 min at 50% amplitude. Then the PLGA@CBD nanoparticles (NPs) resulting were washed with deionized water for three times. The nanoparticles were separated by centrifugation and freeze-dried for subsequent use.

Nanoparticles preparation was optimized using Design Expert software (Version 13), The concentration of PLGA (X_1) and the concentration of PVA (X_2) were selected as independent variables based on preliminary studies, with loading content and nanoparticle shape (Y) as the response variable collectively. To depict the interrelationship between independent and response variables, the obtained data and model were fitted using 3D surface plots [29].

Sample characterization

Nanoparticles structural and morphological features were observed using images obtained on a SU8100 Ultra-High Resolution Scanning Electron Microscope (SEM, Hitachi) and Transmission Electron Microscopy (TEM, Thermo) operated at an accelerating voltage. Nanoparticles size and distribution were acquired by Zetasizer Nano ZS90 (DLS). Each nanoparticle system was measured three times. The powder X-Ray Diffraction (XRD) was recorded on a Rigaku Smartlab SE diffractometer. The Fourier Transform Infrared Spectroscopy (FT-IR) was collected on a Thermo Scientific Nicolet iS20 spectro photometer using KBr pellets.

Drug Loading Capability (DLC)

Dissolve 2mg of the PLGA@CBD nanoparticles (NPs) sample in acetonitrile and sonicate for 30 min under ice bath to break the emulsion completely. The CBD content was quantitatively determined by high performance liquid chromatography (HPLC), and the standard curve of the CBD solution was established in the concentration range of 10−100 μg/mL. The DLC was calculated using the following equations:

$$DLC\ (\%) = \frac{W_1}{W_t} \times 100\%$$

PHARMACEUTICA ANALYTICA ACTA

Subject Area(s):

Subject Area(s): **PHARMACEUTICA ANALYTICA ACTA**

Where: DLC is the drug loading capability, W_1 is the weight of the drug loaded in the nanoparticles and W_t is the total weight of the nanoparticles.

Determination of anti-bacterial activity

Disk-diffusion method: The *S. aureus* suspensions in logarithmic growth phase were diluted to the concentration of 10^8 CFU/mL, and then 1 mL bacterial suspension was mixed with 9 mL agar medium. After solidification, 3 drug-sensitive sheets were placed in each plate and subsequently 30 μL CBD solution, nanoparticles, and blank nanoparticles were added for the three strains of *S. aureus*, respectively. The inhibition zone sizes of each formulation in agar plate were determined after incubation at 37°C for 16-18 h.

Minimum Inhibitory Concentration (MIC) and Minimum Bactericidal Concentration (MBC): The antibacterial activity of the PLGA@CBD was studied using the broth dilution technique as recommended by CLSI. Briefly, serial dilutions nanoparticles and native cannabidiol in sterile water were prepared in 96-well plate. Then *S. aureus* were added to each pore to achieve a final inoculum of 1×10^6 CFU/mL. Then the Optical Density (OD) at a wavelength of 600 nm (OD600) of the bacterial suspension was measured. The MIC of cannabidiol was defined as the lowest concentration inhibiting visible growth of bacteria after 24 h incubation of the cultures at 37°C. MBC was the lowest concentration without visible bacterial growth on LB agar plates at 37°C for 16 h. Each concentration was tested in triplicate.

Bacteria growth curves: The bacteria growth curves of cannabidiol solution and nanoparticles against *S. aureus* were established by plotting time versus ODs (OD 600 nm). Serial dilutions nanoparticles in sterile water were prepared in 96-well plates. Then the *S. aureus* from a mid-log phase culture were added to LB broth to give a starting inoculum of 10^6 CFU/mL. The 96-well plate was incubated at 37°C and derived bacteria growth curves by observing ODs for 12 consecutive hours.

***In vitro* time-kill curve study:** The drugs were prepared to obtain the concentrations corresponding to $1 \times$ MIC, $3\times$ MIC, $5\times$ MIC, in short, the drug concentrations were 6, 18 and 30 μg/mL. The drugs were placed in a release tube and then the tubes were placed in a water bath shaker at 37°C and gently shaken at 100 r/min; 100 uL of supernatant was removed at the specified time, added to an equal volume of the *S. aureus* from a mid-log phase culture of 10^6 CFU/mL.

The antibacterial rate was calculated by observing ODs for 12 hours using the following equation:

$$R\,(\%) = \frac{OD_0 - OD_1}{OD_0} \times 100\%$$

Where: R represents the inhibition rate, OD_1 is the OD of the experimental group, OD_0 is the OD of the blank group.

Determination of adhesion of nanoparticles to bacteria: The diluted nanoparticles were put into the liquid medium containing the *S. aureus* of logarithmic growth phase of 10^6 CFU/mL at the final cannabidiol concentrations of 12 μg/mL, the liquid culture were fixed by glutaraldehyde after incubation for 30, 60, 120min, respectively and then observed whether the composite nanosystems were adsorbed on the surface of bacteria by SEM.

Results and Discussion

Synthesis of PLGA@CBD nanoparticles

The concentration of PLGA and PVA strongly affect the relevant characteristics of nanoparticles as shown in figure 1B. To optimize the parameters, we evaluated the influence of the concentration PLGA (X_1) and PVA (X_2) on the loading content and nanoparticle shape (Y) (**Table S1**). The Y response variables were best fitted by the quadratic model. The equation depicting the relation between the independent and response variables derived using multiple regression analysis is expressed as follows:

$$Y = 19.21 + 2.02X_1 + 14.85X_2 + 0.89X_1X_2 - 0.046X_1{}^2 - 9.33X_2{}^2$$

Summary statistics of the analysis of variance (ANOVA) results (**Table S2**) indicate that Y was significantly influenced by X_1, X_2. PLGA affects the shape of nanoparticles. When PLGA concentration is 10 g/L, the nanoparticles were not smooth and complete. When PVA concentration is 5 g/L, the nanoparticles were seriously aggregated, which affects the load content of nanoparticles (**Figure S1**).

Sample characterization

The synthesis illustration for a simple synthetic strategy of PLGA@CBD nanoplatform and its' application in antibacterial treatment were displayed in Scheme 1. As illustrated, PLGA@CBD nanoparticles were synthesized successfully through
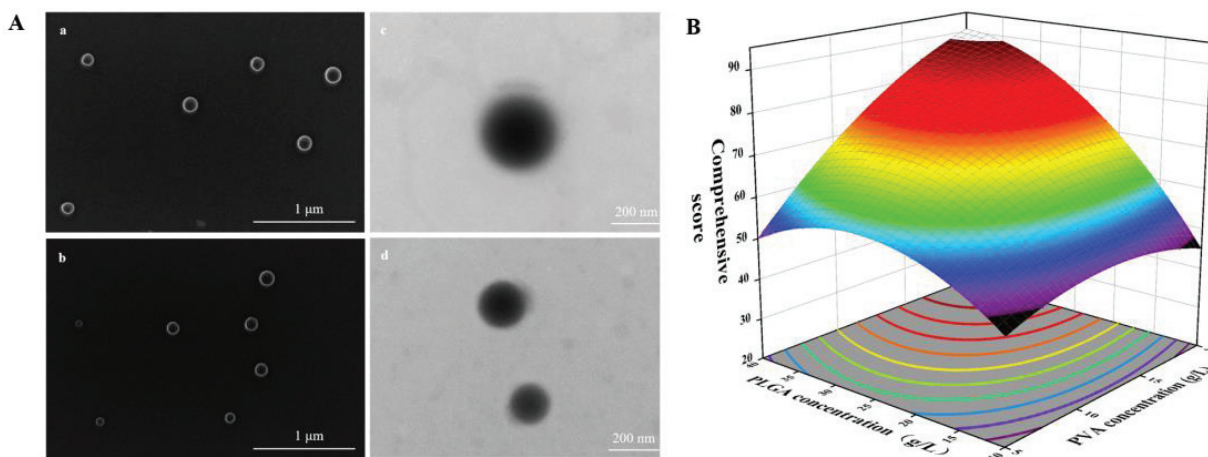
Figure 1 (A) SEM images of PLGA (a, 1 μm), PLGA@CBD (b,1 μm) and TEM images of PLGA (c, 200 nm), PLGA@CBD (d, 200 nm). (B) Response surface plot showing the combined effects of X1 and X2 on Y.

a one-step self-assembly mechanism and CBD were encapsulated inside the PLGA carrier. Beside the antimicrobial activity were characterized *in vitro*. The materials were synthesized and morphologically observed by Scanning Electron Microscopy (SEM) and Transmission Electron Microscopy (TEM). As can be seen in figure 1A, the SEM images of PLGA, PLGA@CBD showed that the average diameters of the synthesized uniformly dispersed nanoparticles were in the range from 150 to 200 nm, respectively (Scheme 1).

The hydrated particle sizes of PLGA, PLGA@CBD were determined by DLS. As shown in figure 2A, the particle size measurements were 281 ± 2.08 nm and 282 ± 4.30 nm, respectively. Each had a narrow size distribution and good water dispersion. The size of PLGA@CBD NPs did not differ much from the size of PLGA materials, which can prove that the drug were encapsulated successfully. The hydrodynamic particle size of the nanoparticles measured by DLS was slightly larger than that observed by SEM, which may be caused by the presence of a hydration layer when the nanoparticles were dispersed in an aqueous solution.

The powder X-Ray Diffraction (XRD) measurement was further performed to determine the crystal structure of CBD, PLGA@CBD, and PLGA. As exhibited in figure 2C, diffraction peak values of CBD are similar to the previous studies [30]. Note the peaks of PLGA@CBD and PLGA were very similar and both are all amorphous, so no spikes were observed in the X-ray diffraction pattern. Moreover, the peak related

with CBD was not found, which further indicated that CBD acted as guest molecules, were embedded inside PLGA.

In addition, the structure of nanoparticles was further qualitatively determined by infrared by FT-IR, as shown in figure 2D, the peaks at 3520 cm^{-1} and 3410 cm^{-1} could be ascribed to the -OH stretching vibrations of CBD, the peak at 3073cm^{-1},1580 cm^{-1},1443 cm^{-1} were from C-H and skeleton of benzene ring stretching, respectively. 1760 cm^{-1} is the characteristic absorption peak of unsaturated ester bond in PLGA molecule and the peak at 3436 cm^{-1} indicates the formation of hydrogen bond between PLGA molecules [31]. while in nanoparticles, due to the limitation of CBD stretching and bending vibration, the characteristic absorption peak of CBD disappears or merges, and the peak of -OH moves to 3440 cm^{-1}, indicating the existence of hydrogen bond between PLGA and CBD. Moreover, the characteristic peak of CBD at 3073 cm^{-1} does not appear in PLGA@CBD, indicating that the internal loading of PLGA on CBD physically masks the characteristic peak. In summary, CBD were successfully loaded in PLGA.

CBD loading efficiency of sample

In order to evaluate the loading and behavior of PLGA@CBD, we first established a standard curve of cannabidiol solution with good linear relationship. It can be seen from figure 2B that the absorbance of CBD shows an increasing trend with increasing concentration. As shown in **table S1**, the highest loading efficiency of PLGA@CBD was achieved when the concentration of PLGA was 40 g/L, and PVA was
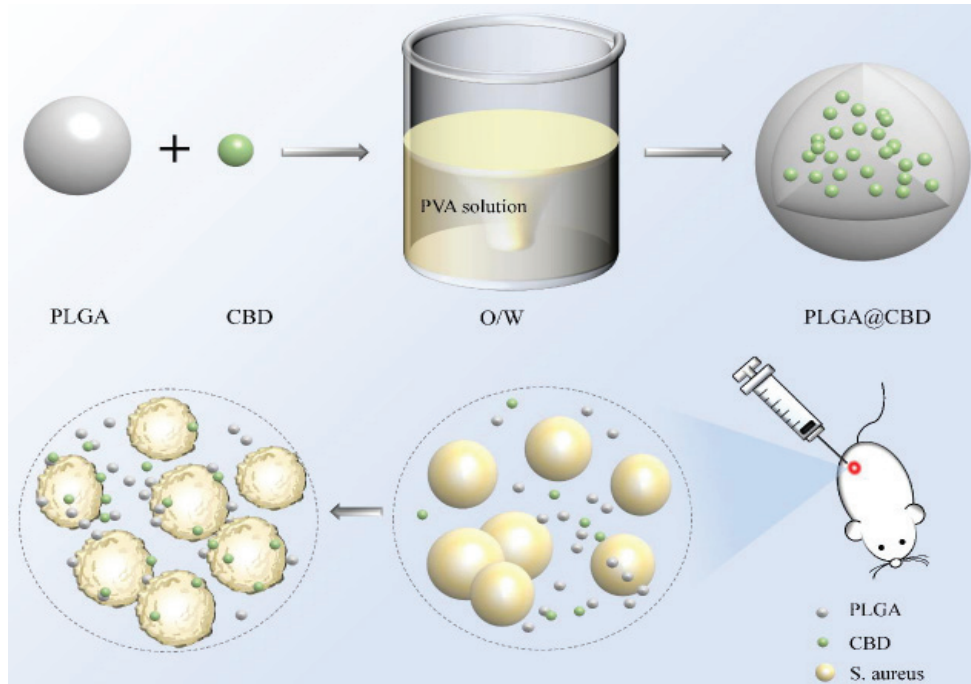
Scheme 1 (A) SEM images of PLGA (a, 1 μm), PLGA@CBD (b,1 μm) and TEM images of PLGA (c, 200 nm), PLGA@CBD (d, 200 nm). (B) Response surface plot showing the combined effects of X1 and X2 on Y.
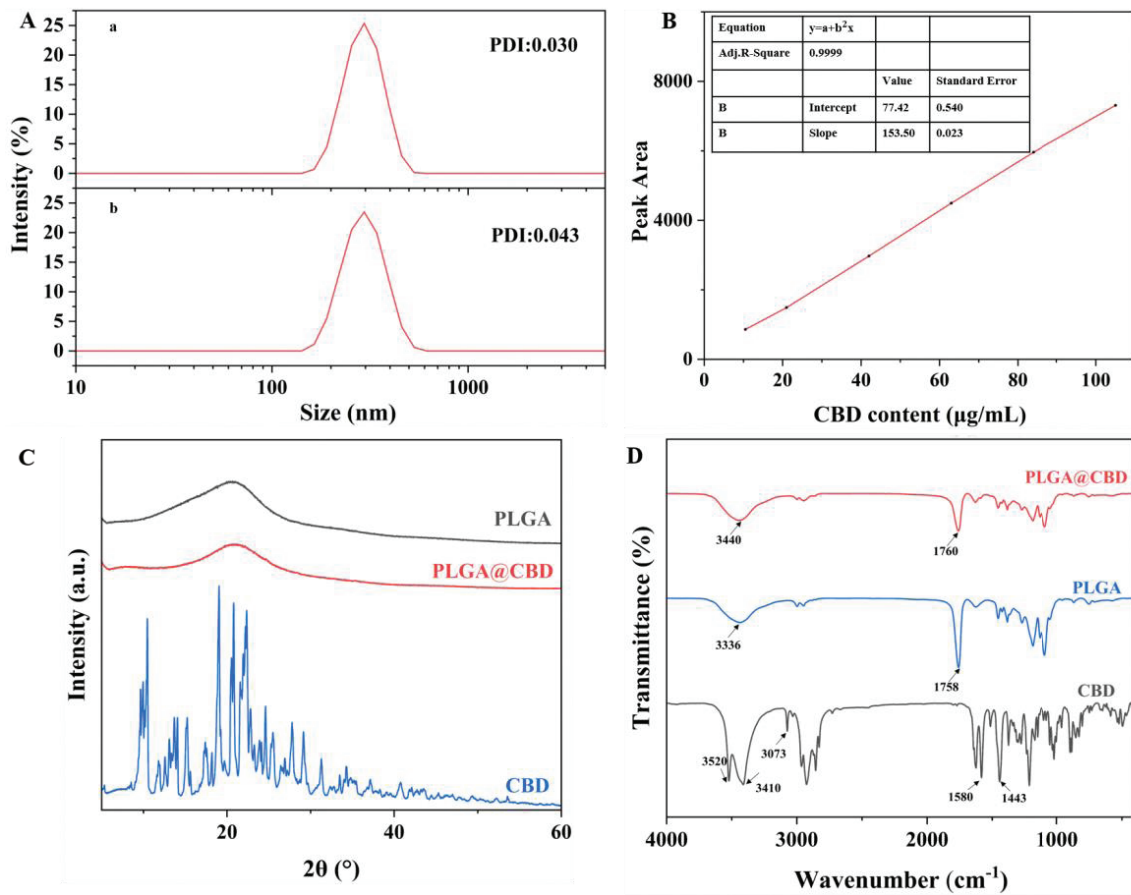

Figure 2 (A) Size distributions measured by DLS of PLGA (a) and PLGA@CBD (b). (B) The standard curve for CBD solutions detected at 210 nm by HPLC. (C) XRD patterns of the PLGA, PLGA@CBD and CBD. (D) FT-IR spectra of as-prepared PLGA@CBD, PLGA and CBD.

2%, the ratio was used for subsequent experiments. In addition, we repeatedly measured the loading efficiency of PLGA@CBD and obtained the result of 16.51 ± 0.66%.

Determination of anti-bacterial activity

The zones of microbial inhibitions: As showed in the figure 3A, the zones of microbial inhibitions of the two different cannabidiol formulations at the same drug concentration were the order: solution > nanoparticle. The zones were 15.03 ± 0.45 mm and 14.55 ± 0.05 mm, respectively (**Table S3**). This might be due to that the drugs were encapsulated inside the material and released slowly, while the cannabidiol solution can diffuse directly, resulting in a smaller bacteriostatic zone of the nanoparticles compared to the solution.

Minimum Inhibitory Concentration (MIC) and Minimum Bactericidal Concentration (MBC): The viability of *S. aureus* treated with PLGA@CBD of different concentrations were evaluated. The MICs of CBD and PLGA@CBD against *S. aureus* were 3 and 6 µg/mL, respectively (**Table S4**). Besides, the MBC of CBD and PLGA@CBD against *S. aureus* were assessed through a plate count assay and found to be the same as the corresponding MIC, 3 and 6 µg/mL, respectively, figure 3C. The same MBC and MIC

resulted in a sterilization rate of 100% for CBD and PLGA@CBD. The results showed that the prepared PLGA@CBD have excellent antibacterial ability. The MIC and MBC of the nanoparticles were higher than natural cannabidiol, which were attributed to the drug encapsulated in the carrier and the slow release compared with cannabidiol solution.

Bacteria growth curves: Figure 3B showed the bacterial growth curve obtained by observing OD value (OD 600 nm) between PLGA@CBD and CBD at different concentrations and the bacterial mixture at an interval of 2 h. There was no significant difference between PLGA@CBD and CBD at low concentration, and when the concentration increased, the bacteriostatic effect of PLGA@CBD was weaker than that of free drug CBD, which was due to the slow drug release of PLGA@CBD nanoparticles. However, when the concentration increased to 6 µg/mL, the growth curves of nanoparticles and free drug showed no signal growth, as shown in the **figure S2**. We observed from growth curves of bacterial solution incubated with different concentrations of PLGA@CBD, the growth curve was the same as free drug CBD at lower concentrations. Bacteria started to grow slowly for the first two hours. In third to eighth hours, the growth curves of CBD entered the log phase, a period featured by exponential multiple growth in terms of the number
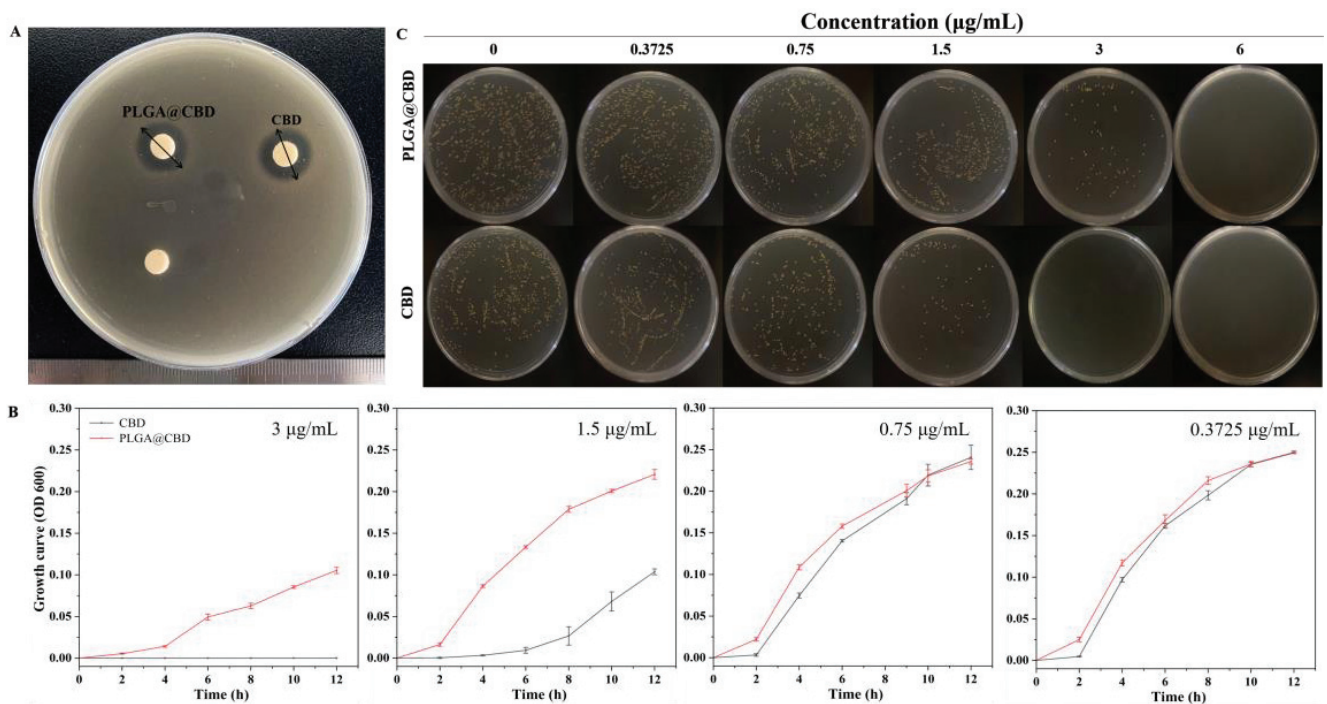

Figure 3 (A) Inhibition zone of PLGA@CBD and PLGA. (B) Growth curves of bacterial solution incubated with different concentrations of PLGA@CBD and CBD. (C) Photographs of bacterial colonies on agar plates.

Subject Area(s): PHARMACEUTICA ANALYTICA ACTA

of *S. aureus*, subsequently the stationary phase was initiated. As the concentration of CBD increases, it delayed the entry of *S. aureus* into the log phase, CBD concentrations up to 3 µg/ml effectively inhibited the growth of *S. aureus* in the first four hours and enter the log phase at fifth to twelfth hours. Meanwhile, the ODs decreased significantly indicating that it stably inhibited the growth of some bacteria. When the concentration continued to increase to 6 µg/ml, the nanoparticles continued to inhibit bacterial growth

steadily, demonstrating that PLGA@CBD inhibits bacterial growth in a concentration–dependent manner. Growth curves of bacterial solution incubated with different concentrations of CBD in **figure S2**.

In vitro time-kill curve study: We explored the inhibition time after the interaction of different concentrations of CBD and PLGA@CBD NPs with *S. aureus*, as shown in the figure 4A, with the increase of CBD concentration, its action time became longer,
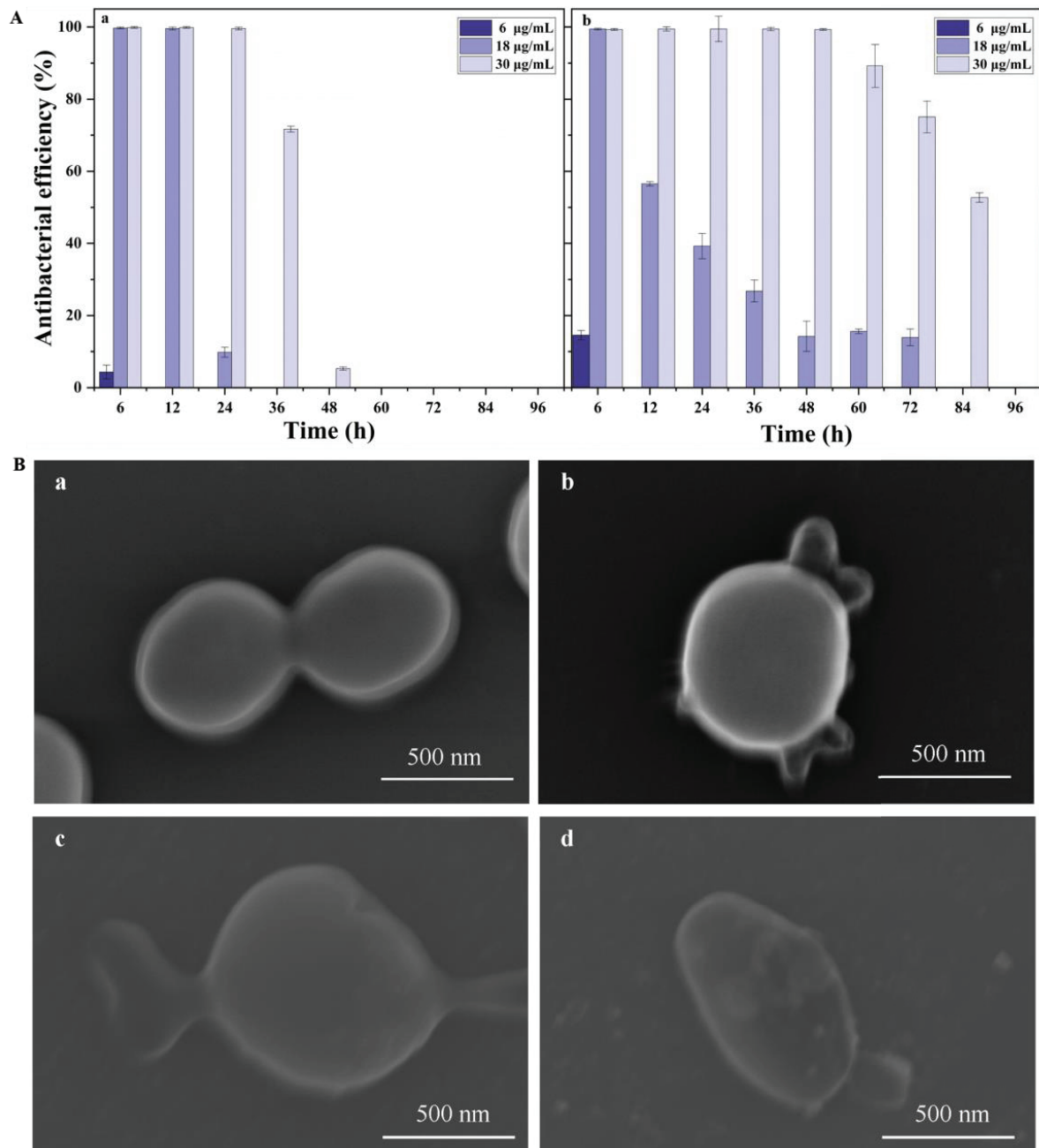

Figure 4 (A) The time-kill curve of CBD solutions (a) and PLGA@CBD nanoparticles (b). (B) SEM images that bacteria and nanoparticles were co-cultured for 0 min (a, 500 nm), 30min (b, 500 nm), 60min (c, 500 nm) and 120min (d, 500 nm).

and the action time of nanoparticles was significantly better than that of CBD solution. After 36 hours, the inhibition rate of the solution at the concentration of 30 μg/ml of CBD decreased significantly and the inhibition rate was only 5.28% at 48 hours, while nanoparticles could still effectively inhibit bacterial and the inhibition rate of PLGA@CBD nanoparticles was 52.68% at 84 h. This was attributed to the long-lasting and stable release of nanoparticles, which enhanced the antibacterial time. In addition, the short action time of free drug CBD is also related to its instability. Studies have shown that CBD is highly unstable, the solvent used has an important influence on the stability of the CBD, CBD is not stable in aqueous medium. And under simulated physiological conditions (pH 7.4 and 37°C), 10% of CBD was degraded within 24 hours [28]. Therefore, PLGA@CBD nanoparticles have superior time killing ability compared with free drugs.

Adhesion of nanoparticles to bacteria: To clarify the long-lasting antibacterial mechanism, bacteria and nanoparticles were co-cultured for 30, 60 and 120 min using SEM. SEM images showed that the nanoparticles were in contact with or absorbed by the bacteria figure 4B, which could affect the integrity of the bacterial cell membrane or increase drug entry into the bacteria. The uptake may be due to the adhesion of the PLGA carrier. Bacterial cell walls and cell membrane structures of untreated CBD-treated bacteria were intact and the cytoplasm was evenly distributed. The morphology of the CBD-treated bacteria changed significantly with the cell integrity being disrupted as the duration of action increased. The bacteria collapsed, making it impossible to maintain its original full form, and after two hours, the contents flowed out. The results were consistent with previous reports suggesting that its antibacterial properties act on the bacterial cell membrane[25]. We still need to continue to explore its possible sites of action, including membrane proteins, membrane lipids, membrane potential, etc.

Conclusion

In this study we have successfully explored a novel self-assembled nanoparticle for the treatment of *S. aureus* infections. The nanoparticles were formed by hydrogen bonding between PLGA and CBD. Compared to simple cannabidiol solutions, the nanoparticles can be adsorbed on the surface of *S. aureus* and therefore show superior sustained antibacterial benefits. This result confirms that we have prepared nanoparticles

that reduce premature drug release and enhance targeted release against *S. aureus*. Thus, the present study could be a fruitful strategy to overcome the therapeutic challenges of *S. aureus* as well as other bacterial infections.

References

1. Cassini A, Högberg LD, Plachouras D, Quattrocchi A, Hoxha A, Simonsen GS, Colomb-Cotinat M, Kretzschmar ME, Devleesschauwer B, Cecchini M, Ouakrim DA, Oliveira TC, Struelens MJ, Suetens C, Monnet DL; Burden of AMR Collaborative Group. Attributable deaths and disability-adjusted life-years caused by infections with antibiotic-resistant bacteria in the EU and the European Economic Area in 2015: a population-level modelling analysis. Lancet Infect Dis. 2019 Jan;19(1):56-66. doi: 10.1016/S1473-3099(18)30605-4. Epub 2018 Nov 5. PMID: 30409683; PMCID: PMC6300481.

2. Richter MF, Drown BS, Riley AP, Garcia A, Shirai T, Svec RL, Hergenrother PJ. Predictive compound accumulation rules yield a broad-spectrum antibiotic. Nature. 2017 May 18;545(7654):299-304. doi: 10.1038/nature22308. Epub 2017 May 10. PMID: 28489819; PMCID: PMC5737020.

3. Sousa MC. New antibiotics target the outer membrane of bacteria. Nature. 2019 Dec;576(7787):389-390. doi: 10.1038/d41586-019-03730-x. PMID: 31844257.

4. Arciola CR, Campoccia D, Montanaro L. Implant infections: adhesion, biofilm formation and immune evasion. Nat Rev Microbiol. 2018 Jul;16(7):397-409. doi: 10.1038/s41579-018-0019-y. PMID: 29720707.

5. Michael CA, Dominey-Howes D, Labbate M. The antimicrobial resistance crisis: causes, consequences, and management. Front Public Health. 2014 Sep 16;2:145. doi: 10.3389/fpubh.2014.00145. PMID: 25279369; PMCID: PMC4165128.

6. Wang LS, Gupta A, Rotello VMJAID. Nanomaterials for the Treatment of Bacterial Biofilms [J]. 2015;2(1):151021155851001.

7. Pelgrift RY, Friedman AJ. Nanotechnology as a therapeutic tool to combat microbial resistance. Adv Drug Deliv Rev. 2013 Nov;65(13-14):1803-15. doi: 10.1016/j.addr.2013.07.011. Epub 2013 Jul 24. PMID: 23892192.

8. Soenen SJ, Rivera-Gil P, Montenegro JM, et al. Cellular toxicity of inorganic nanoparticles: Common aspects and guidelines for improved nanotoxicity evaluation. 2011;6(5):446-65.

9. Bee SL, Hamid ZAA, Mariatti M, et al. Approaches to Improve Therapeutic Efficacy of Biodegradable PLA/PLGA Microspheres: A Review [J]. Polymer Reviews. 2018;58(3):495-536.

10. McManamon C, de Silva JP, Delaney P, Morris MA, Cross GLW. Characteristics, interactions and coating adherence of heterogeneous polymer/drug coatings for biomedical devices. Mater Sci Eng C Mater Biol Appl. 2016 Feb;59:102-108. doi: 10.1016/j.msec.2015.09.103. Epub 2015 Oct 1. PMID: 26652354.

Subject Area(s): PHARMACEUTICA ANALYTICA ACTA

11. Kim JK, Go EJ, Ko KW, Oh HJ, Han J, Han DK, Park W. PLGA Microspheres Containing Hydrophobically Modified Magnesium Hydroxide Particles for Acid Neutralization-Mediated Anti-Inflammation. Tissue Eng Regen Med. 2021 Aug;18(4):613-622. doi: 10.1007/s13770-021-00338-z. Epub 2021 Apr 20. PMID: 33877618; PMCID: PMC8325726.

12. Zhang E, Osipova N, Sokolov M, Maksimenko O, Semyonkin A, Wang M, Grigartzik L, Gelperina S, Sabel BA, Henrich-Noack P. Exploring the systemic delivery of a poorly water-soluble model drug to the retina using PLGA nanoparticles. Eur J Pharm Sci. 2021 Sep 1;164:105905. doi: 10.1016/j.ejps.2021.105905. Epub 2021 Jun 8. PMID: 34116175.

13. Grune C, Zens C, Czapka A, Scheuer K, Thamm J, Hoeppener S, Jandt KD, Werz O, Neugebauer U, Fischer D. Sustainable preparation of anti-inflammatory atorvastatin PLGA nanoparticles. Int J Pharm. 2021 Apr 15;599:120404. doi: 10.1016/j.ijpharm.2021.120404. Epub 2021 Feb 26. PMID: 33647413.

14. Cao J, Yuan L, Long CJAMUSETH. Preparation and in vitro Biocompatibility of Heparin-loaded PLGA Nanoparticles [J]. 2012.

15. Shah P, Sarolia J, Vyas B, Wagh P, Ankur K, Kumar MA. PLGA Nanoparticles for Nose to Brain Delivery of Clonazepam: Formulation, Optimization by 32 Factorial Design, In Vitro and In Vivo Evaluation. Curr Drug Deliv. 2021;18(6):805-824. doi: 10.2174/1567201817666200708115627. PMID: 32640955.

16. Su Y, Zhang B, Sun R, Liu W, Zhu Q, Zhang X, Wang R, Chen C. PLGA-based biodegradable microspheres in drug delivery: recent advances in research and application. Drug Deliv. 2021 Dec;28(1):1397-1418. doi: 10.1080/10717544.2021.1938756. PMID: 34184949; PMCID: PMC8248937.

17. Kumar SS, Gopalakrishnan G, Gowrishankar NLJRJOP, et al. Design, Optimization and in vitro Characterization of Dasatinib loaded PLGA Nano carrier for Targeted cancer therapy: A Preliminary Evaluation [J]. 2021;(14-4).

18. Fagherazzi EV, Garcia VA, Maurmann N, Bervanger T, Halmenschlager LH, Busato SB, Hallak JE, Zuardi AW, Crippa JA, Schröder N. Memory-rescuing effects of cannabidiol in an animal model of cognitive impairment relevant to neurodegenerative disorders. Psychopharmacology (Berl). 2012 Feb;219(4):1133-40. doi: 10.1007/s00213-011-2449-3. Epub 2011 Aug 26. PMID: 21870037.

19. Chetia S, Borah G. Δ 9-Tetrahydrocannabinol Toxicity and Validation of Cannabidiol on Brain Dopamine Levels: An Assessment on Cannabis Duplicity. Nat Prod Bioprospect. 2020 Oct;10(5):285-296. doi: 10.1007/s13659-020-00263-z. Epub 2020 Aug 28. PMID: 32860199; PMCID: PMC7520491.

20. Appiah-Kusi E, Petros N, Wilson R, Colizzi M, Bossong MG, Valmaggia L, Mondelli V, McGuire P, Bhattacharyya S. Effects of short-term cannabidiol treatment on response to social stress in subjects at clinical high risk of developing psychosis. Psychopharmacology (Berl). 2020 Apr;237(4):1121-1130. doi: 10.1007/s00213-019-05442-6. Epub 2020 Jan 8. PMID: 31915861; PMCID: PMC7113209.

21. Etges T, Karolia K, Grint T, Taylor A, Lauder H, Daka B, Wright S. An observational postmarketing safety registry of patients in the UK, Germany, and Switzerland who have been prescribed Sativex® (THC:CBD, nabiximols) oromucosal spray. Ther Clin Risk Manag. 2016 Nov 11;12:1667-1675. doi: 10.2147/TCRM.S115014. PMID: 27956834; PMCID: PMC5113923.

22. Pauli CS, Conroy M, Vanden Heuvel BD, Park SH. Cannabidiol Drugs Clinical Trial Outcomes and Adverse Effects. Front Pharmacol. 2020 Feb 25;11:63. doi: 10.3389/fphar.2020.00063. PMID: 32161538; PMCID: PMC7053164.

23. Feldman M, Smoum R, Mechoulam R, et al. Antimicrobial potential of endocannabinoid and endocannabinoid-like compounds against methicillin-resistant Staphylococcus aureus [J]. 2018;8(1):17696.

24. Appendino G, Gibbons S, Giana A, Pagani A, Grassi G, Stavri M, Smith E, Rahman MM. Antibacterial cannabinoids from Cannabis sativa: a structure-activity study. J Nat Prod. 2008 Aug;71(8):1427-30. doi: 10.1021/np8002673. Epub 2008 Aug 6. PMID: 18681481.

25. Król E, de Sousa Borges A, da Silva I, Polaquini CR, Regasini LO, Ferreira H, Scheffers DJ. Antibacterial activity of alkyl gallates is a combination of direct targeting of FtsZ and permeabilization of bacterial membranes. Front Microbiol. 2015 Apr 29;6:390. doi: 10.3389/fmicb.2015.00390. PMID: 25972861; PMCID: PMC4413848.

26. Li H, Chang SL, Chang TR, et al. Inclusion complexes of cannabidiol with β-cyclodextrin and its derivative: Physicochemical properties, water solubility, and antioxidant activity [J]. 2021;334:116070.

27. Fraguas-Sánchez AI, Fernández-Carballido A, Martin-Sabroso C, Torres-Suárez AI. Stability characteristics of cannabidiol for the design of pharmacological, biochemical and pharmaceutical studies. J Chromatogr B Analyt Technol Biomed Life Sci. 2020 Aug 1;1150:122188. doi: 10.1016/j.jchromb.2020.122188. Epub 2020 May 22. PMID: 32506012.

28. Ramazani F, Chen W, van Nostrum CF, Storm G, Kiessling F, Lammers T, Hennink WE, Kok RJ. Strategies for encapsulation of small hydrophilic and amphiphilic drugs in PLGA microspheres: State-of-the-art and challenges. Int J Pharm. 2016 Feb 29;499(1-2):358-367. doi: 10.1016/j.ijpharm.2016.01.020. Epub 2016 Jan 12. PMID: 26795193.

29. Zhang C, Jia R, Dong Y, et al. Preparation and characterization of poly (3-hydroxybutyrate-co-3-hydroxyhexanoate) microspheres for controlled release of buprofezin [J]. 2019.

30. Lv P, Zhang D, Guo M, et al. Structural analysis and cytotoxicity of host-guest inclusion complexes of cannabidiol with three native cyclodextrins [J]. 2019.

31. Wang H, Ng LF, Chen HL, et al. Study on preparation of PLGA-CS composite membrane scaffold and its characteristics in vitro [J]. 2009.